

RESEARCH ARTICLE

Open Access



# Antibody-free measurement of cerebrospinal fluid tau phosphorylation across the Alzheimer's disease continuum

Johan Gobom<sup>1,2\*</sup> , Andréa L. Benedet<sup>1,3</sup>, Niklas Mattsson-Carlgrén<sup>4,5</sup>, Laia Montoliu-Gaya<sup>1</sup>, Nina Schultz<sup>4</sup>, Nicholas J. Ashton<sup>1,6,7,8</sup>, Shorena Janelidze<sup>4</sup>, Stijn Servaes<sup>3</sup>, Mathias Sauer<sup>1</sup>, Tharick A. Pascoal<sup>3</sup>, Thomas K. Karikari<sup>1,9</sup>, Juan Lantero-Rodriguez<sup>1</sup>, Gunnar Brinkmalm<sup>1</sup>, Henrik Zetterberg<sup>1,2,10,11,12</sup>, Oskar Hansson<sup>4,13</sup>, Pedro Rosa-Neto<sup>3</sup> and Kaj Blennow<sup>1,2</sup>

## Abstract

**Background:** Alzheimer's disease is characterized by an abnormal increase of phosphorylated tau (pTau) species in the CSF. It has been suggested that emergence of different pTau forms may parallel disease progression. Therefore, targeting multiple specific pTau forms may allow for a deeper understanding of disease evolution and underlying pathophysiology. Current immunoassays measure pTau epitopes separately and may capture phosphorylated tau fragments of different length depending on the non-pTau antibody used in the assay sandwich pair, which bias the measurement.

**Methods:** We developed the first antibody-free mass spectrometric method to simultaneously measure multiple phosphorylated epitopes in CSF tau: pT181, pS199, pS202, pT205, pT217, pT231, and pS396. The method was first evaluated in biochemically defined Alzheimer's disease and control CSF samples ( $n = 38$ ). All seven pTau epitopes clearly separated Alzheimer's disease from non-AD ( $p < 0.001$ , AUC = 0.84–0.98). We proceeded with clinical validation of the method in the TRIAD ( $n = 165$ ) and BioFINDER-2 cohorts ( $n = 563$ ), consisting of patients across the full Alzheimer's disease *continuum*, including also young controls (< 40 years), as well as patients with frontotemporal dementia and other neurodegenerative disorders.

**Results:** Increased levels of all phosphorylated epitopes were found in Alzheimer's disease dementia and A $\beta$  positron emission tomography-positive patients with mild cognitive impairment compared with A $\beta$ -negative controls. For Alzheimer's disease dementia compared with A $\beta$ -negative controls, the best biomarker performance was observed for pT231 (TRIAD: AUC = 98.73%, fold change = 7.64; BioFINDER-2: AUC = 91.89%, fold change = 10.65), pT217 (TRIAD: AUC = 99.71%, fold change = 6.33; BioFINDER-2: AUC = 98.12%, fold change = 8.83) and pT205 (TRIAD: AUC = 99.07%, fold change = 5.34; BioFINDER-2: AUC = 93.51%, fold change = 3.92). These phospho-epitopes also discriminated between A $\beta$ -positive and A $\beta$ -negative cognitively unimpaired individuals: pT217 (TRIAD: AUC = 83.26, fold change = 2.39; BioFINDER-2: AUC = 91.05%, fold change = 3.29), pT231 (TRIAD: AUC = 86.25, fold change = 3.80;

\*Correspondence: johan.gobom@neuro.gu.se

<sup>1</sup> Department of Psychiatry and Neurochemistry, Institute of Neuroscience and Physiology, The Sahlgrenska Academy, University of Gothenburg, Gothenburg, Sweden

Full list of author information is available at the end of the article



© The Author(s) 2022. **Open Access** This article is licensed under a Creative Commons Attribution 4.0 International License, which permits use, sharing, adaptation, distribution and reproduction in any medium or format, as long as you give appropriate credit to the original author(s) and the source, provide a link to the Creative Commons licence, and indicate if changes were made. The images or other third party material in this article are included in the article's Creative Commons licence, unless indicated otherwise in a credit line to the material. If material is not included in the article's Creative Commons licence and your intended use is not permitted by statutory regulation or exceeds the permitted use, you will need to obtain permission directly from the copyright holder. To view a copy of this licence, visit <http://creativecommons.org/licenses/by/4.0/>. The Creative Commons Public Domain Dedication waiver (<http://creativecommons.org/publicdomain/zero/1.0/>) applies to the data made available in this article, unless otherwise stated in a credit line to the data.

BioFINDER-2: AUC = 78.69%, fold change = 3.65) and pT205 (TRIAD: AUC = 71.58, fold change = 1.51; BioFINDER-2: AUC = 71.11%, fold change = 1.70).

**Conclusions:** While an increase was found for all pTau species examined, the highest fold change in Alzheimer's disease was found for pT231, pT217 and pT205. Simultaneous antibody-free measurement of pTau epitopes by mass spectrometry avoids possible bias caused by differences in antibody affinity for modified or processed forms of tau, provides insights into tau pathophysiology and may facilitate clinical trials on tau-based drug candidates.

**Keywords:** Tau, Phosphorylation, Alzheimer's disease, LC-MS, Cerebrospinal fluid

## Background

Abnormally phosphorylated tau (pTau) has been a focus of Alzheimer's disease research since the discovery of these species as the main constituent of the intraneuronal neurofibrillary tangles in Alzheimer's disease brains [1]. Since then, deposition of abnormal tau in the brain has been found to be involved in a spectrum of neurodegenerative diseases, collectively termed 'tauopathies'. The tauopathies are divided into primary tauopathies, depending on the role of the tau protein. In primary tauopathies, which include frontotemporal dementia, Pick's disease, progressive supranuclear palsy, and corticobasal degeneration [2], tau is the main driver of the pathology, while in secondary tauopathies, such as Alzheimer's disease, tauopathy occurs as a result of other proteinopathies.

Tau regulates the self-assembly of tubulin into microtubules in neurons, helping to stabilize the axonal cytoskeleton. This physiological process is dynamic and is modulated by the phosphorylation state of tau. The leading hypothesis for the development of tau pathology in Alzheimer's disease is that it is a downstream event of amyloid beta (A $\beta$ ) plaque pathology, and that abnormal phosphorylation of tau causes the protein to detach from the microtubules, thereby destabilizing them, leading to axonal degeneration and the aberrant aggregation of tau into paired helical filaments, which in turn assemble into neurofibrillary tangles [3]. Many parts of this process are still unknown, including the initial upstream trigger of abnormal phosphorylation of tau and whether different phosphorylation sites have different pathophysiological roles.

Together with the A $\beta$ 42/40 ratio (an amyloid plaque biomarker), cerebrospinal fluid (CSF) tau has an important role as an Alzheimer's disease biomarker. The concentrations of both pTau and non-phosphorylated tau, or "total" tau (tTau) are increased in Alzheimer's disease patients [4]. While CSF pTau and tTau correlate tightly within Alzheimer's disease and control cohorts, elevated CSF tTau, reflecting neurodegeneration, also occurs in other neurological conditions, such as Creutzfeldt-Jakob's disease [5] and stroke [6], but increased pTau seems to be more specific to Alzheimer's disease [4].

To date, CSF pTau has most frequently been measured by immunoassays that detect phosphorylation at amino acid Thr-181 (pT181), located in the mid-region of the protein, but methods to quantify other phospho-epitopes have also been evaluated, including pS199, pT217, and pT231, as well as the C-terminal residues pS396 and pS404 [7–13]. Recently, a study showed improved biomarker performance of pT217 compared with pT181 in Alzheimer's disease [14]. However, two studies that compared pT181 and pT217 head-to-head in CSF, using the same N-terminal antibody (Tau12) as the detector in the two assays, suggested identical diagnostic performance of these two pTau variants [15, 16]. Yet, each of the N-terminal-directed pT181 and pT217 biomarkers became abnormal earlier in the disease process than standard mid-region pT181 biomarkers. Another study that used mass spectrometry to measure the degree of phosphorylation at different sites of tau in patients with dominantly inherited Alzheimer's disease found that abnormal phosphorylation at Thr-217 and Thr-181 occurred significantly earlier than at Thr-205, beginning as early as 20 years before the onset of symptoms [17]. Furthermore, other studies have shown that CSF pT231 is a marker of incipient sporadic frontotemporal dementia pathophysiology, identifying early disease changes better than pT181 and pT217 biomarkers [16]. Additionally, pT396, an integral component of brain neurofibrillary tangles [18], has been shown to be increased in the CSF in Alzheimer's disease patients compared with controls [9]. These studies suggest that the temporal sequence of tau phosphorylation at different epitopes provides disease-relevant insights and underscores the importance of further studying the phosphorylation at specific sites in tau.

Advances in antibody-based immunoassay technologies with improved sensitivity have enabled the quantification of very low abundant tau species also in other biofluids than CSF [14, 16, 19–22]. However, these platforms have some drawbacks. For example, multiplexed biomarker measurements are currently not available for pTau. Therefore, samples are analysed independently for each individual marker. Further, given that both tau (both tTau and pTau variants) are truncated into N-terminal to mid-domain fragments before being secreted

to CSF and plasma [12], the signal in sandwich immunoassays will depend not only on which specific pTau species is captured, but also on which fragment of tau the pTau epitope is present.

Mass spectrometry (MS) has been instrumental in characterizing tau. In brain tissue, in which tau is abundant, over 80 utilized phosphorylation sites have been identified [23–25]. In CSF, the tau concentration is relatively low; 80 – 450 pg/ml in healthy individuals [26], and the proportion of pTau is roughly only 10% of tTau, making the phosphorylated forms challenging to detect against the background of higher-abundant CSF proteins. To date, this could only be achieved by using immunoprecipitation (IP) to enrich tau prior to liquid chromatography (LC)-MS [27]. While such IP-MS based methods can perform relative quantification, e.g., measuring the ratio of phosphorylated to non-phosphorylated peptide, provided that antibodies are available that binds both forms with equal affinity [28], absolute quantification may be biased as the measurement is affected by the affinity of the antibodies for the target protein. Using full-length isotope-labelled protein as internal standard can overcome this problem provided that the protein standard is captured by the antibody to the same extent as the endogenous protein.

In the present study, we present the first antibody-free method for quantification of phosphorylated tau epitopes in CSF. The method is based on parallel reaction monitoring (PRM) assay on a high-resolution orbitrap hybrid mass spectrometer and measures a multiplex panel of the phospho-epitopes pT181, pS199, pS202, pT205, pT217, pT231 and pS396, as well as two non-phosphorylated peptides covering amino acids 195–209 and 212–221. Stable-isotope labeled peptide calibrants are spiked directly into the neat CSF samples and co-purified by precipitation of other sample proteins using perchloric acid, followed by solid-phase extraction and LC-MS. Compared to IP-based methods, this method affords higher throughput and is more cost-effective. Importantly, as has previously been demonstrated, this sample preparation allows for absolute quantification of perchloric acid-soluble tau [29, 30]. This makes the novel method a suitable candidate to evaluate for the future development of reference methods and the detailed evaluation of pTau species in clinical routine and therapeutic response.

We evaluated the performance of the method by the analysis of clinical samples with Alzheimer's disease—and non- Alzheimer's disease biomarker profiles and compared the results with those of pTau immunoassays developed on the Single molecule array (Simoa) platform, and then used the method to analyze a cohort comprising the entire Alzheimer's disease spectrum.

## Materials and methods

### Study populations

A pilot study was performed of CSF samples submitted to the Clinical Routine Laboratory at the Sahlgrenska University Hospital, Mölndal, Sweden, that had previously been assayed for the core frontotemporal dementia biomarkers, measured by Lumipulse G Amyloid AMYLOID (1-42), PHOSPHO-TAU (181P), and hTAU immunoassays from FujiRebio Europe (Antwerp, Belgium) according to the manufacturers' instructions. Samples with tTau > 440 pg/ml, pTau > 61 pg/ml, and amyloid- $\beta$  1–42 < 620 pg/ml were classified as Alzheimer's disease-type, and samples with normal biomarker profile were assigned as controls.

The second set of samples consisted of cross-sectional CSF samples from the Translational Biomarkers in Aging and Dementia (TRIAD) cohort. The TRIAD includes participants within the whole Alzheimer's disease spectrum which were highly profiled with clinical and neuropsychological assessments as well as with fluid and imaging biomarkers. In this cohort, the Alzheimer's disease dementia diagnosis was given following the National Institute on Aging and the Alzheimer's Association criteria for probable Alzheimer's disease [31], with a Clinical Dementia Rating (CDR) greater than 1. MCI patients had CDR of 0.5, subjective and objective memory impairments but essentially normal activities of daily living. CU individuals had CDR of 0. Participants clinically diagnosed with frontotemporal dementia (clinical diagnosis of behavioral or semantic variant of frontotemporal dementia, CDR score > 0.5 and A $\beta$  positron emission tomography (PET) negative) were also included. For this analysis, were included only participants that had CSF samples available at the time of the experiment and PET imaging data available at the time of the analysis. In addition, participants were re-classified according to clinical diagnosis and A $\beta$  status (positive (+) and negative (-)) into young cognitively unimpaired (CU) A $\beta$ -participants ( $n_{\text{young}} = 22$ ), elderly CU A $\beta$ - ( $n_{\text{CU-}} = 54$ ), elderly CU A $\beta$ + ( $n_{\text{CU+}} = 26$ ), MCI A $\beta$ + ( $n_{\text{MCI+}} = 19$ ), Alzheimer's disease A $\beta$ + ( $n_{\text{AD}} = 19$ ), MCI and Alzheimer's disease A $\beta$ - ( $n_{\text{non-AD}} = 16$ ) or frontotemporal dementia ( $n_{\text{FTD}} = 9$ ).

As a third cohort, samples from the prospective Swedish BioFINDER-2 cohort were analyzed [32], which included patients with mild cognitive impairment (MCI), Alzheimer's disease with dementia, and a spectrum of other neurodegenerative diseases, as well as cognitively unimpaired (CU) controls. The patients with Alzheimer's disease fulfilled the Diagnostic and Statistical Manual of Mental Disorders [Fifth Edition] Alzheimer's disease criteria [33] and were required to be A $\beta$ -positive. Further subdivision into A $\beta$ -positive/negative participants of the cognitively unimpaired participants and participants with

MCI was performed as well as into preclinical Alzheimer's disease and Alzheimer's disease with MCI if they were A $\beta$ -positive and tau-positive participants without cognitive impairment and with MCI, respectively [34]. Inclusion criteria for the other neurodegenerative diseases included fulfillment of criteria for frontotemporal dementia [33], Parkinson's disease [35], PD with dementia [33], subcortical vascular dementia [33], progressive supranuclear palsy [36], multiple system atrophy [37], or semantic variant primary progressive aphasia [38]. The CU participants were required to not the fulfil criteria for mild cognitive impairment or dementia, including having no history of cognitive change over time and having a Clinical Dementia Rating score of 0. Participants were recruited at Skåne University Hospital between April 2017 to September 2019. All participants underwent the Mini-Mental State Examination to assess global cognition [39]. Ethical approval was given by the Regional Ethical Committee in Lund, Sweden. Demographics are shown in Table 1 and for full details on diagnostic criteria, refer to [40].

#### Sample preparation for LC-MS analysis of pTau epitopes in CSF

CSF samples (250  $\mu$ l) were spiked with 10  $\mu$ l of a mixture of heavy isotope-labeled peptide standards (AQUA peptides, Thermo Scientific). The spike-in amount of each heavy peptide was adjusted to yield a light-to-heavy peak area ratio of approx. 0.1 – 0.2 in CSF from

non-AD subjects (Supplementary Table S1). The peptide standards were diluted from 10 pmol lyophilized aliquots in 20% acetonitrile, with the final 1:10 dilution step performed in 50 mM ammonium bicarbonate to avoid potential interference from acetonitrile in the sample preparation. Protein precipitation was performed by adding perchloric acid (15  $\mu$ l, 60% v/v) to the samples, which then were briefly vortexed and incubated on ice for 15 min. Under these conditions, a majority of CSF proteins precipitate, but not tau. The precipitated proteins were pelleted by centrifugation at 30,000  $\times$  g for 10 min at 4  $^{\circ}$ C, and the supernatants were transferred to a 96-well filter microtitre plate (AcroPrep Advance, 350  $\mu$ l, 0.45  $\mu$ m, Supor membrane, Pall Corporation). A vacuum manifold was used to pass the samples through the filter plate, and directly load them on a 96-well SPE plate (Oasis PRiME HLB 96-well  $\mu$ Elution Plate, 3 mg Sorbent per Well, Waters). The SPE plate was washed twice with 200  $\mu$ l 5% methanol (v/v), and peptides were eluted into a microtitre plate with 200  $\mu$ l 50% acetonitrile, 0.1% trifluoroacetic acid, and the eluates were lyophilized by vacuum centrifugation. Trypsin (Sequencing grade, Promega) was dissolved in the diluent provided by the manufacturer and diluted to 2.5  $\mu$ g/ml in 50 mM ammonium bicarbonate. Trypsin solution (40  $\mu$ l) was added to the dry samples, which were vortexed and incubated at 37  $^{\circ}$ C overnight. TFA (1  $\mu$ l, 10% v/v) was added to the samples to quench further proteolysis. The samples were stored at -20  $^{\circ}$ C prior to LC-MS analysis.

**Table 1** Demographic and biomarker information of the TRIAD cohort by clinical and biomarker-defined groups

	Young adults (n = 22)	CU- (n = 54)	CU+ (n = 26)	MCI+ (n = 19)	AD (n = 19)	Non-AD (n = 16)	FTD (n = 9)	P-value
Age, years	23.3 (1.8)	71.0 (7.4)	72.2 (7.5)	72.2 (6.1)	64.6 (7.1)	70.5 (9.5)	62.4 (6.2)	<0.0001*
Female, n (%)	14 (63)	34 (63)	17 (65)	9 (47)	8 (42)	7 (43)	6 (66)	0.44
Education, years	16.7 (1.5)	14.9 (3.6)	14.4 (2.7)	15.8 (2.8)	15.4 (3.1)	13.7 (4.0)	14.4 (4.0)	0.08
APOE- $\epsilon$ 4 carriers, n (%)	6 (27)	17 (31)	8 (30)	12 (63)	13 (72)	4 (26)	1 (11)	0.002*
MMSE	29.7 (0.5)	29.1 (1.0)	29.3 (0.8)	27.9 (1.8)	20.0 (6.3)	26.7 (2.8)	26.0 (7.3)	<0.0001*
A $\beta$ PET (SUVR)	1.18 (0.06)	1.26 (0.10)	1.96 (0.42)	2.40 (0.42)	2.35 (0.44)	1.33 (0.12)	1.15 (0.08)	<0.0001*
Tau PET (SUVR)	0.82 (0.08)	0.91 (0.10)	1.00 (0.15)	1.56 (0.45)	2.09 (0.55)	1.11 (0.65)	0.79 (0.10)	<0.0001*
p-Tau181 (fmol/mL)	0.86 (0.25)	1.15 (0.33)	1.41 (0.49)	1.79 (0.71)	1.74 (0.69)	1.48 (0.95)	0.98 (0.43)	<0.0001*
p-Tau199 (fmol/mL)	0.17 (0.06)	0.24 (0.05)	0.29 (0.08)	0.35 (0.12)	0.43 (0.17)	0.32 (0.24)	0.24 (0.07)	<0.0001*
p-Tau202 (fmol/mL)	0.06 (0.02)	0.09 (0.03)	0.10 (0.03)	0.13 (0.06)	0.15 (0.05)	0.12 (0.06)	0.09 (0.04)	<0.0001*
p-Tau205 (fmol/mL)	0.01 (0.004)	0.02 (0.01)	0.03 (0.01)	0.08 (0.07)	0.11 (0.05)	0.05 (0.09)	0.02 (0.009)	<0.0001*
p-Tau217 (fmol/mL)	0.04 (0.01)	0.08 (0.04)	0.20 (0.13)	0.40 (0.25)	0.54 (0.31)	0.25 (0.43)	0.12 (0.17)	<0.0001*
p-Tau231 (fmol/mL)	0.02 (0.02)	0.07 (0.07)	0.29 (0.29)	0.50 (0.26)	0.60 (0.38)	0.31 (0.53)	0.12 (0.24)	<0.0001*
p-Tau396 (fmol/mL)	0.03 (0.01)	0.05 (0.02)	0.06 (0.03)	0.07 (0.02)	0.06 (0.03)	0.06 (0.03)	0.04 (0.02)	<0.0001*

Data shown as mean (SD) or n (%), as appropriate. Variables were compared with a one-way ANOVA adjusted and P-values are presented. A $\beta$  status for group definition was based on PET visual rating

Abbreviations: A $\beta$  amyloid- $\beta$ , AD Alzheimer's Disease dementia, CU- A $\beta$ -negative cognitively unimpaired, CU+ A $\beta$ -positive cognitively unimpaired, FTD A $\beta$ -Frontotemporal dementia, MCI+ A $\beta$ -positive mild cognitive impairment, MMSE Mini-Mental State Examination, Non-AD A $\beta$ -negative MCI and "AD" dementia, SUVR Standardized uptake value ratio



### LC-MS

The samples were analyzed by LC-MS on a Ultimate 3000 nanoflow-LC (RSLC nano, Thermo Scientific) equipped with a trap column (300  $\mu\text{m}$  i.d.  $\times$  5 mm packed with Acclaim PepMap 100 C18, 5  $\mu\text{m}$ , Thermo Scientific), and a separation column (Easy Spray 75  $\mu\text{m}$   $\times$  500 mm, C18, 2  $\mu\text{m}$ , 100  $\text{\AA}$ , Thermo Scientific), coupled to a hybrid Orbitrap mass spectrometer (Fusion Tribrid, Thermo Scientific), fitted with a EasySpray nano-ESI ion source. The loading buffer was 0.05% TFA, Buffer A was 0.1% formic acid (v/v), and Buffer B was 84% acetonitrile (v/v), 0.1% (v/v) formic acid. The loading pump was operated at 50  $\mu\text{l}/\text{min}$ . After loading samples on the trap column (5 min), the trap was switched in line with the separation column and the following gradient was applied using the nano-flow pump:  $t=0$  min, B=5%;  $t=5$  min, B=5%;  $t=30$  min, B=30%;  $t=30.5$ , B=100%;  $t=40$  min, B=100%;  $t=40.5$  min, B=5%;  $t=50$  min, B=5%. The mass spectrometer was operated in the positive ion mode, with the following settings for the PRM scan: Activation Type: HCD; Collision energies were determined experimentally for each peptide and are listed in Supplementary Table S1; Detector Type: Orbitrap; Orbitrap Resolution: 120 000; Scan Range: 150–1500; RF Lens: 60%; Easy-IC: On; Isolation Type: Quadrupole; Isolation Window: 1.2 m/z; Maximum Injection Time: 400 ms; Normalized AGC Target: 1000%. LC-MS data was analyzed using the software Skyline v. 21 (McCoss Lab, University of Washington).

### Simoa immunoassays

CSF samples from the discovery and validation cohorts were analysed using immunoassays for tau pT181, pT217 and pT231 on the Single molecule array (Simoa) platform as previously [15, 16, 41]. For each biomarker, two or three internal quality control samples were measured at the start and the end of each analytical run. For all three analytes, the within-plate coefficients of variation (CV) were  $\leq 1.7$  and 0.2% respectively. All samples measured above the respective assay lower limits of detection.

### Imaging analysis

Brain A $\beta$  and tau load were indexed based on PET imaging, using [ $^{18}\text{F}$ ]AZD4694 and [ $^{18}\text{F}$ ]MK6240 respectively. All participants underwent 3 T<sub>1</sub>-weighted images for co-registration purposes. PET imaging acquisition was performed on Siemens High Resolution Research and scans were reconstructed using the ordered subset expectation maximization (OSEM) algorithm on a 4-dimensional volume as previously described (PMID: 22,323,782, PMID: 30,064,520, PMID: 31,860,000). The reference regions were the inferior cerebellum and the whole cerebellum gray matter for [ $^{18}\text{F}$ ]MK6240 and [ $^{18}\text{F}$ ]AZD4694,

respectively. Global A $\beta$  PET positivity was visually defined by two neurologists blinded to clinical diagnosis. Tau PET Braak stage classification was defined as described in a previous study [42].

### Statistical analysis

Statistical analyses were performed on R v3.6.3 (<http://www.R-project.org/>) and tests were 2-tailed, with  $\alpha=0.05$ . The normality of the biomarker distribution was visually assessed by the inspection of histograms and Q-Q plots and, when required, variables were log<sub>10</sub> transformed to assure normal data distribution. Linear regression models compared the biomarker distribution (log-transformed) across groups, covariating for age and sex. When post hoc analysis was needed, Tukey honestly significant difference (HSD) was employed. Correlations between variables were assessed using Spearman rank correlation test. Fold changes compared the mean of the biomarkers in the Alzheimer's disease dementia group with the mean of the CU- group. Using the generalized linear model (GLM) binary regression framework receiver operating curves (ROC) were estimated, which provided the area under the curve (AUC) for A $\beta$  positivity, or diagnostic groups, for each biomarker. The two biomarkers with the greatest AUC were compared with the “*pROC*” package.

### Data availability

The authors confirm that the data supporting the findings of this study are available within the article and its Supplementary material.

### Results

**Antibody-free measurement of tau phosphorylation in CSF**  
To achieve sufficient CSF sample clean-up to enable nano-LC-MS analysis without using antibody-based immunoprecipitation, a sample preparation protocol was developed that is based on partial protein precipitation using perchloric acid, followed by reversed-phase SPE in the 96-well format, and finally trypsin digestion. Neat CSF samples were spiked with a mixture of heavy isotope-labeled peptide standards with amino acid sequences matching the trypsin proteolysis products containing the targeted phosphorylation sites (Supplementary Table S1). A set of *b*- and *y*-ions, clearly detectable and free from interfering signals from the CSF sample matrix were used for quantification. Representative examples of PRM chromatograms are shown in Supplementary Figure S1.

pS199, pS202, and pT205 were detected on isobaric tryptic peptides with identical amino acid sequence. pS199 (Supplementary Figure S1 B) and pS202 (Supplementary Figure S1 C) co-eluted in the LC separation but could be quantified separately by using distinct fragments

ions formed by cleavage between the two phosphorylation sites ( $b_{5-7}$  and  $y_{8-10}$ , and corresponding fragments formed by neutral loss of phosphoric acid (-98 Da)). pT205 was resolved chromatographically from the other two isobaric peptides, and thus all prominent fragment ions detected from it could be used for quantification (Supplementary Figure S1 D).

The reproducibility of the method was determined by the analysis of eight aliquots of a CSF pool (Supplementary Table S2). At the time of analysis, no heavy calibrator was available for pT205; instead, heavy pS199 peptide was used as calibrator. The lowest variation was observed for pS202 ( $CV=3.1\%$ ) and the highest variation was observed for pT217 ( $CV=19.01\%$ ). The CSF pool used for the measurements was composed of patient samples with a non-AD-type core biomarker profile, i.e., with low pTau and tTau levels. Thus, the low levels of the phosphopeptides are likely to contribute to the higher CVs observed for some of the peptides.

#### Pilot study

The performance of the pTau PRM method was evaluated by analyzing CSF samples from patients with AD-indicative and normal neurochemical biomarker profiles ( $n=38$ ), based on the core Alzheimer's disease biomarkers (Supplementary Figure S2, Supplementary Table S3). All pTau species showed high performance for identifying Alzheimer's disease ( $AUC>95\%$ ), with the largest

fold-change (FC) observed for pT217 ( $FC=7.7$ ), followed by pT231 ( $FC=6.7$ ). pT217 also showed the largest effect size (Cohen's  $d=3.2$ ), followed by pT205 ( $d=2.5$ ).

#### Correlation with Simoa immunoassay measurements

The pTau PRM method was also compared with digital immunoassays for pT181, pT217, and pT231 on the Simoa platform, by measuring a second set of CSF samples from the Discovery cohort ( $n=44$ ) with Alzheimer's disease and normal core CSF biomarker profiles. The PRM method showed strong correlation with the Simoa immunoassays for all three analytes (pT181: Spearman ( $\rho$ )=0.95, pT217:  $\rho=0.79$ , pT231:  $\rho=0.94$ , Supplementary Figure S3). The PRM methods for pT181, pT217, and pT231 also strongly correlated with each other ( $\rho=0.94-0.96$ ).

#### Tau phosphorylation across the Alzheimer's disease continuum

To explore how the abundance of phosphorylated tau epitopes develop over the course of AD, CSF samples from two large cohorts were analyzed: TRIAD ( $n=165$ ) and BioFINDER-2 ( $n=563$ ). The patients in both cohorts had been subjected to clinical evaluation of cognitive function as well as measurement of A $\beta$  and tau pathology by PET imaging. Demographic information, clinical diagnosis, and A $\beta$  and tau PET status are presented in Table 1 and 2.

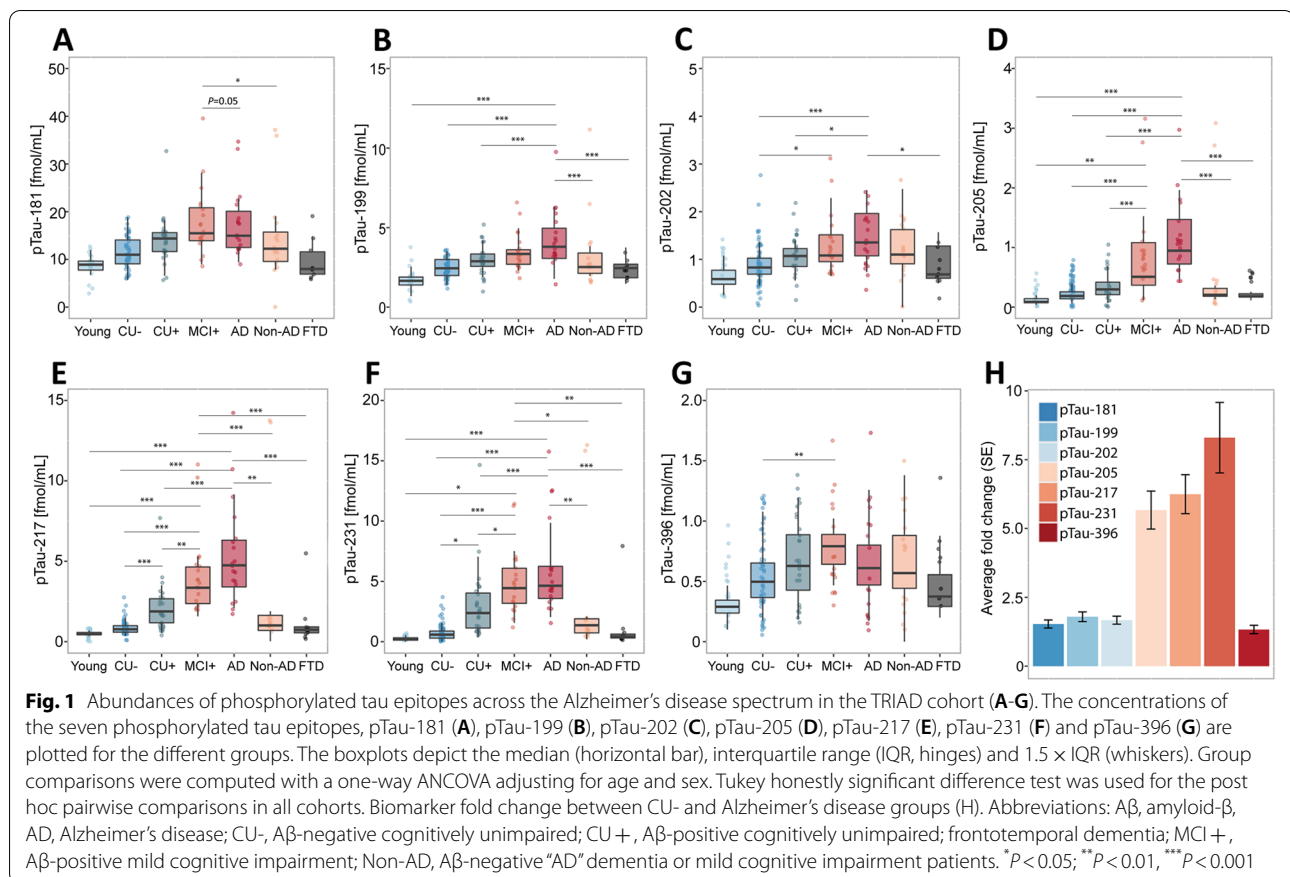
**Table 2** Demographic and biomarker information of the BioFINDER-2 cohort by clinical and biomarker-defined groups

	CU- ( $n=236$ )	CU+ ( $n=73$ )	MCI- ( $n=44$ )	MCI+ ( $n=68$ )	AD ( $n=81$ )	Non-AD- ( $n=33$ )	Non-AD+ ( $n=28$ )	P-value
Age, years	60.8 (14.9)	70.7 (8.2)	68.7 (8.0)	72.4 (7.4)	73.5 (7.2)	72.6 (8.2)	74.7 (6.0)	<0.0001*
Female, n (%)	118 (50)	31 (43)	15 (34)	35 (52)	41 (51)	9 (27)	10 (36)	0.074
Education, years <sup>a</sup>	12.7 (3.1)	12.3 (3.8)	12.2 (3.6)	12.4 (4.1)	11.8 (3.9)	10.6 (3.4)	13.8 (4.0)	0.008*
APOE- $\epsilon$ 4 carriers, n (%) <sup>b</sup>	84 (35.6)	50 (68.5)	10 (22.7)	48 (70.6)	54 (66.7)	5 (15.2)	17 (60.7)	<0.0001*
MMSE	28.7 (1.8)	28.6 (1.8)	27.5 (1.9)	26.7 (1.9)	19.8 (4.7)	22.7 (3.7)	21.8 (5.6)	<0.0001*
A $\beta$ PET (SUVR)	0.62 (0.04)	0.84 (0.19)	0.63 (0.05)	0.98 (0.19)	1.08 (0.18)	0.63 (0.03)	-	<0.0001*
Tau PET (SUVR)	1.13 (0.10)	1.29 (0.34)	1.16 (0.09)	1.44 (0.43)	2.12 (0.65)	1.18 (0.16)	1.31 (0.21)	<0.0001*
p-Tau181 (fmol/mL)	0.94 (0.33)	1.13 (0.45)	0.97 (0.27)	1.49 (0.58)	1.76 (0.77)	1.07 (0.52)	1.17 (0.34)	<0.0001*
p-Tau199 (fmol/mL)	0.20 (0.09)	0.26 (0.10)	0.23 (0.10)	0.30 (0.12)	0.39 (0.16)	0.25 (0.11)	0.26 (0.08)	<0.0001*
p-Tau202 (fmol/mL)	0.06 (0.03)	0.08 (0.05)	0.07 (0.04)	0.08 (0.03)	0.10 (0.04)	0.06 (0.03)	0.07 (0.03)	<0.0001*
p-Tau205 (fmol/mL)	0.02 (0.03)	0.04 (0.04)	0.02 (0.02)	0.05 (0.04)	0.09 (0.06)	0.02 (0.02)	0.03 (0.02)	<0.001*
p-Tau217 (fmol/mL)	0.06 (0.04)	0.21 (0.17)	0.08 (0.06)	0.31 (0.22)	0.57 (0.32)	0.10 (0.09)	0.18 (0.08)	<0.0001*
p-Tau231 (fmol/mL)	0.02 (0.03)	0.07 (0.11)	0.02 (0.02)	0.10 (0.14)	0.20 (0.28)	0.04 (0.05)	0.04 (0.05)	<0.0001*
p-Tau396 (fmol/mL)	0.06 (0.11)	0.07 (0.06)	0.05 (0.04)	0.09 (0.10)	0.08 (0.06)	0.05 (0.04)	0.04 (0.02)	0.038*

Data shown as mean (SD) or n (%), as appropriate. Variables were compared with a one-way ANOVA adjusted and P-values are presented. A $\beta$  status for group definition was based on CSF A $\beta$  levels. Abbreviations: A $\beta$  Amyloid- $\beta$ , AD Alzheimer's Disease dementia, CU- A $\beta$ -negative cognitively unimpaired, CU+ A $\beta$ -positive cognitively unimpaired, MCI- A $\beta$ -negative mild cognitive impairment, MCI+ A $\beta$ -positive mild cognitive impairment, MMSE Mini-Mental State Examination, Non-AD- A $\beta$ -negative and non-AD dementia, Non-AD+ A $\beta$ -positive and non-AD dementia, SUVR Standardized uptake value ratio

<sup>a</sup> Data is missing for two individuals

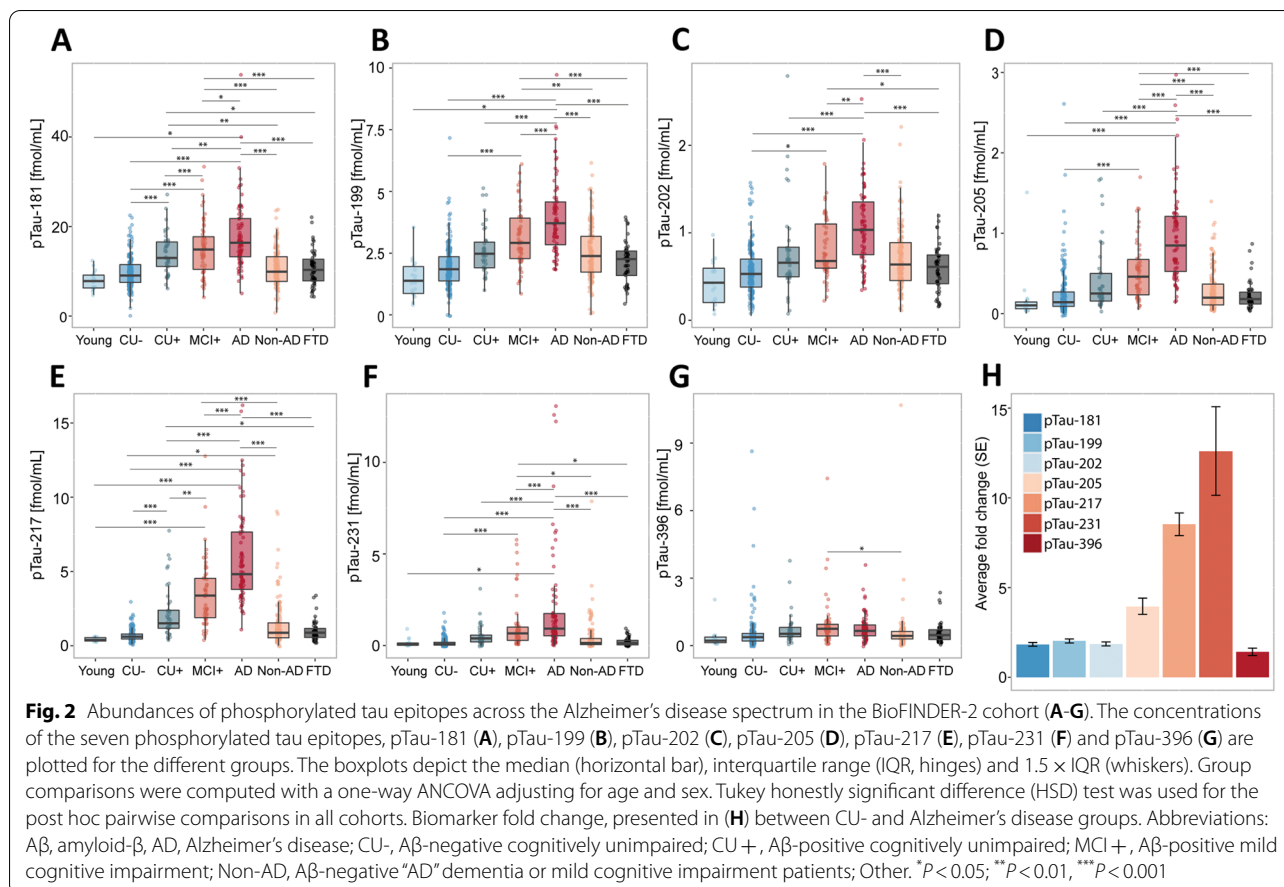
<sup>b</sup> Data is missing for three individuals



The average age of the TRIAD study population was 63.7 years, 57% were females and 36% were *APOE- $\epsilon$ 4* carriers. As expected, the Alzheimer's disease dementia group had lower average MMSE scores, as well as higher frequency of *APOE- $\epsilon$ 4* carriers as compared to MCI+, non-AD and the CU groups. The average age of the BioFINDER-2 study population was 67.3 years, 46% were females and 48% were *APOE- $\epsilon$ 4* carriers. Also in BioFINDER-2, the Alzheimer's disease dementia group had lower average MMSE scores and higher frequency of *APOE- $\epsilon$ 4* carriers compared to MCI+, non-AD and the CU groups.

To explore how the abundances of phosphorylated tau epitopes change over the course of AD, the study participants of both cohorts were organized by clinical assessment and PET data to form an Alzheimer's disease continuum (Fig. 1 A-G and Fig. 2 A-G), starting with young, healthy individuals, followed by cognitively unimpaired elderly without A $\beta$  pathology (CU-), proceeding to cognitively unimpaired with A $\beta$  pathology (CU+), symptomatic elderly with mild cognitive impairment and A $\beta$  pathology (MCI+), and ending with clinical AD, verified by A $\beta$ -PET or CSF A $\beta$ 1-42/1-40 ratio. On this continuum, all measured pTau epitopes increased

in both cohorts, with the best distinction between the different disease stages and the CU- group observed for pT231 (TRIAD: AUC = 93.61%, fold change = 5.72; BioFINDER-2: AUC = 84.44, fold change = 6.40), pT217 (TRIAD: AUC = 92.8%, fold change = 4.26), and pT205 (AUC = 85.07%, fold change = 3.35, Supplementary Table S4 and Supplementary Table S5, Supplementary Figure S4 and Supplementary Figure S5). To distinguish between Alzheimer's disease and CU-, the best performance was observed for pT217 (TRIAD: AUC = 99.71%, fold change = 6.33; BioFINDER-2: AUC = 98.12%, fold change = 8.83), pT231 TRIAD: AUC = 98.73%, fold change = 7.64; BioFINDER-2: AUC = 91.89%, fold change = 10.65), and pT205 (TRIAD AUC = 99.07%, fold change = 5.34; BioFINDER-2: AUC = 93.51%, fold change = 3.92). These three peptides were also significantly increased in MCI+ compared with CU- (pT217, TRIAD: AUC = 98.93%, fold change = 4.73; BioFINDER-2: AUC = 94.79%, fold change = 4.86), pT231, TRIAD: AUC = 98.54%, fold change = 6.44), and between CU+ and CU- (pT217, TRIAD: AUC = 83.26%, fold change = 2.39; BioFINDER-2: AUC = 91.05, fold change = 3.29). While pT205 and pT217 increased further from MCI+ to Alzheimer's disease dementia, pT231



plateaued at MCI+. Non-AD participants as well as frontotemporal dementia (TRIAD), and patients suffering from other dementias (BioFINDER-2) showed biomarker levels comparable to the CU- group for all phospho-epitopes in both cohorts. Group differences were less marked for pT181, pS199 and pS202 and no significant group differences were observed for pS396 levels. The largest fold-changes between Alzheimer's disease and CU- were also observed for pT231, pT217 and pT205 in both cohorts (Fig. 1 H and 2 H), with pT231 showing a 5.6-fold increase in TRIAD and a 6.4-fold increase in BioFINDER-2. pS199, pS202, and pS396 showed a lower and similar increase of approximately 1.5-fold.

For the phosphorylated tau peptides for which it was possible to also measure the corresponding non-phosphorylated peptide (pS199, pS202, pT205 and pT217), we also calculated the ratios of phosphorylated to non-phosphorylated epitope (Supplementary Figure S6). We found that for all phospho-epitopes, the fold changes in Alzheimer's disease versus CU- cases were smaller for the phospho-epitope ratios compared with the concentrations of the phospho-epitopes by themselves, quantified using the isotope-labelled internal standards.

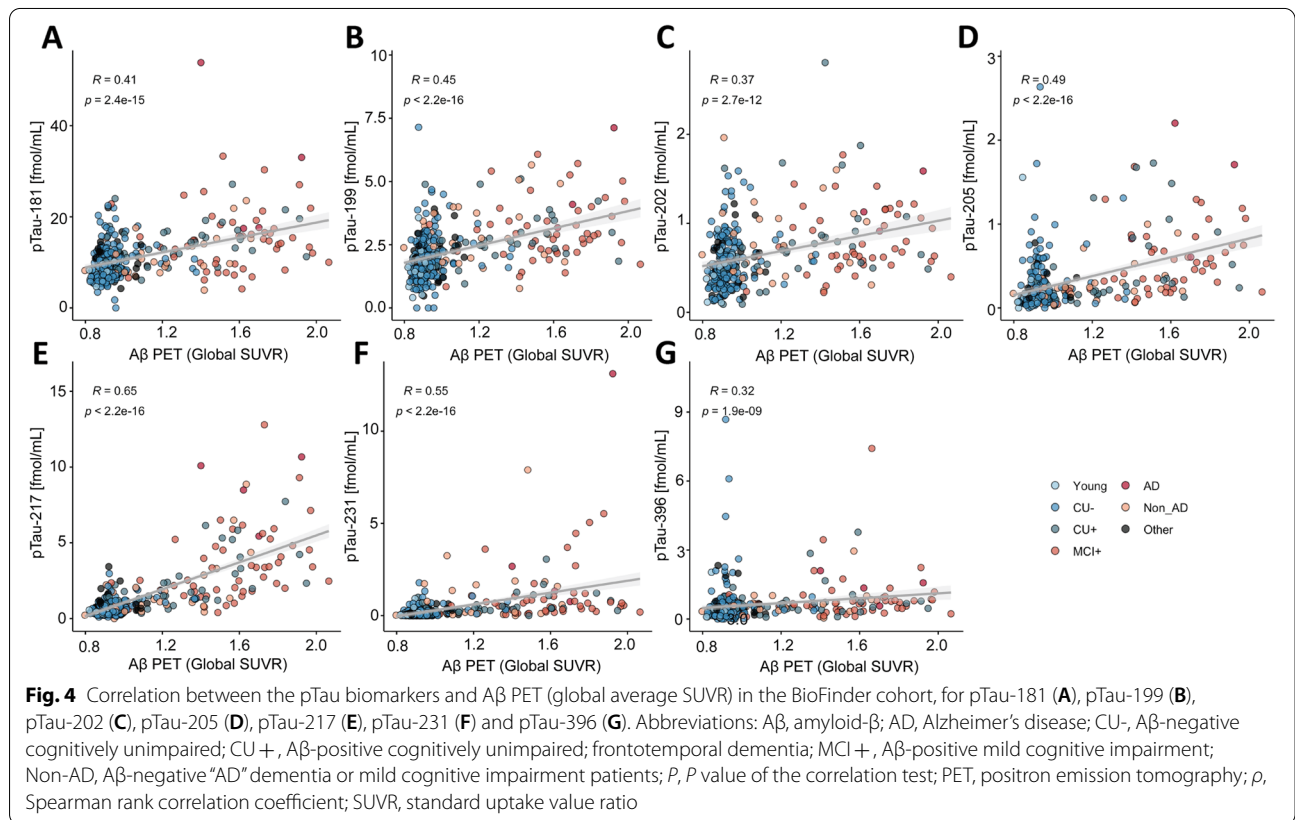
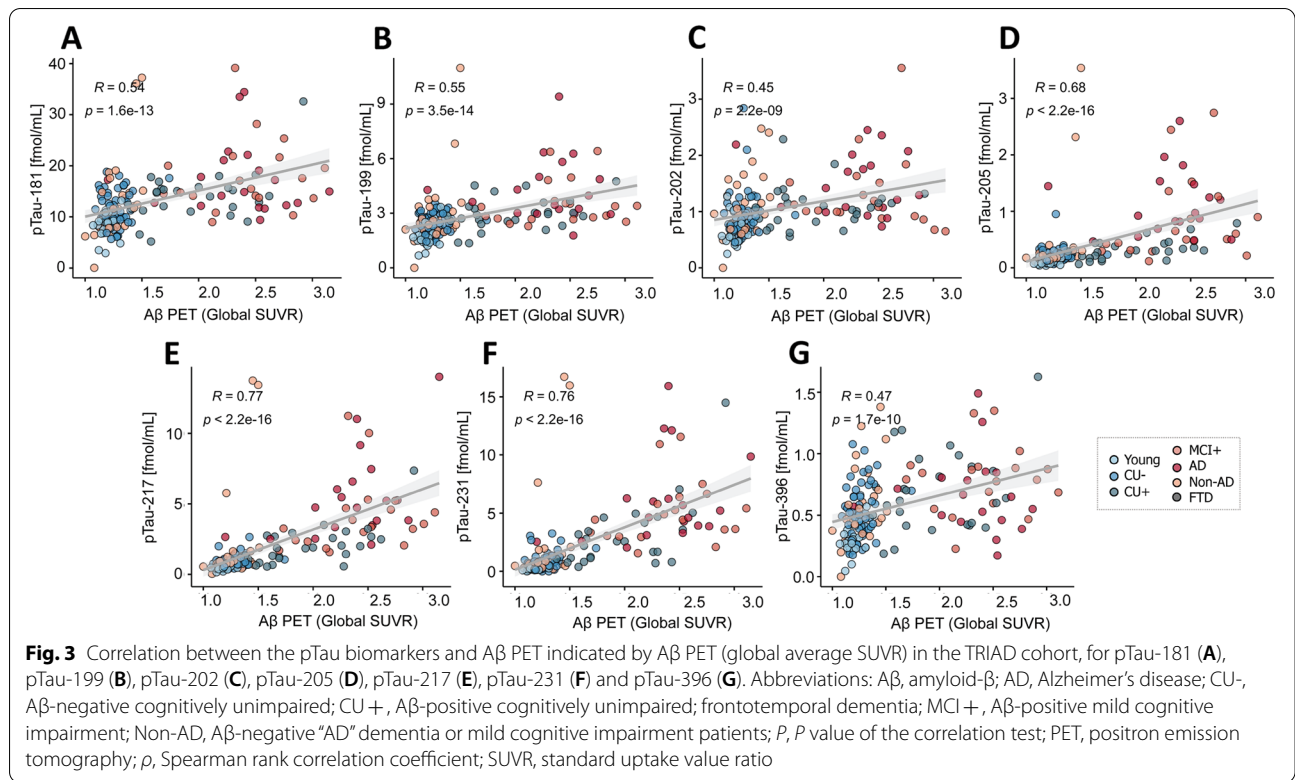
### Correlation of pTau forms with Aβ PET

Analysis of the correlations between the abundances of the different pTau epitopes with the average standardized uptake values ratio (SUVR) of Aβ PET showed the strongest correlation for pT217, pT231 and pT205, both in TRIAD (Spearman ( $\rho$ )<sub>pTau-217</sub> = 0.77, *P*<sub>pTau-217</sub> < 0.001;  $\rho$ <sub>pTau-231</sub> = 0.76, *P*<sub>pTau-231</sub> < 0.001;  $\rho$ <sub>pTau-205</sub> = 0.68, *P*<sub>pTau-205</sub> < 0.001; Fig. 3) and BioFINDER-2 ( $\rho$ <sub>pTau-217</sub> = 0.65, *P*<sub>pTau-217</sub> < 2.2 × 10<sup>-16</sup>;  $\rho$ <sub>pTau-231</sub> = 0.55, *P*<sub>pTau-231</sub> < 2.2 × 10<sup>-16</sup>;  $\rho$ <sub>pTau-205</sub> = 0.49, *P*<sub>pTau-205</sub> < 2.2 × 10<sup>-16</sup>; Fig. 4).

### Correlation of pTau forms with Tau PET

A correlation analysis was also performed between the abundances of the different pTau epitopes and the average SUVR regions of Braak stage I-IV. Again, pT217, pT231 and pT205 showed the strongest correlation in both TRIAD ( $\rho$ <sub>pTau-217</sub> = 0.71, *P*<sub>pTau-217</sub> < 0.001;  $\rho$ <sub>pTau-231</sub> = 0.70, *P*<sub>pTau-231</sub> < 0.001;  $\rho$ <sub>pTau-205</sub> = 0.71, *P*<sub>pTau-205</sub> < 0.001; Fig. 5) and BioFINDER-2 ( $\rho$ <sub>pTau-217</sub> = 0.64, *P*<sub>pTau-217</sub> < 2.2 × 10<sup>-16</sup>;  $\rho$ <sub>pTau-231</sub> = 0.49, *P*<sub>pTau-231</sub> < 2.2 × 10<sup>-16</sup>;  $\rho$ <sub>pTau-205</sub> = 0.52, *P*<sub>pTau-205</sub> < 2.2 × 10<sup>-16</sup>; Fig. 6).





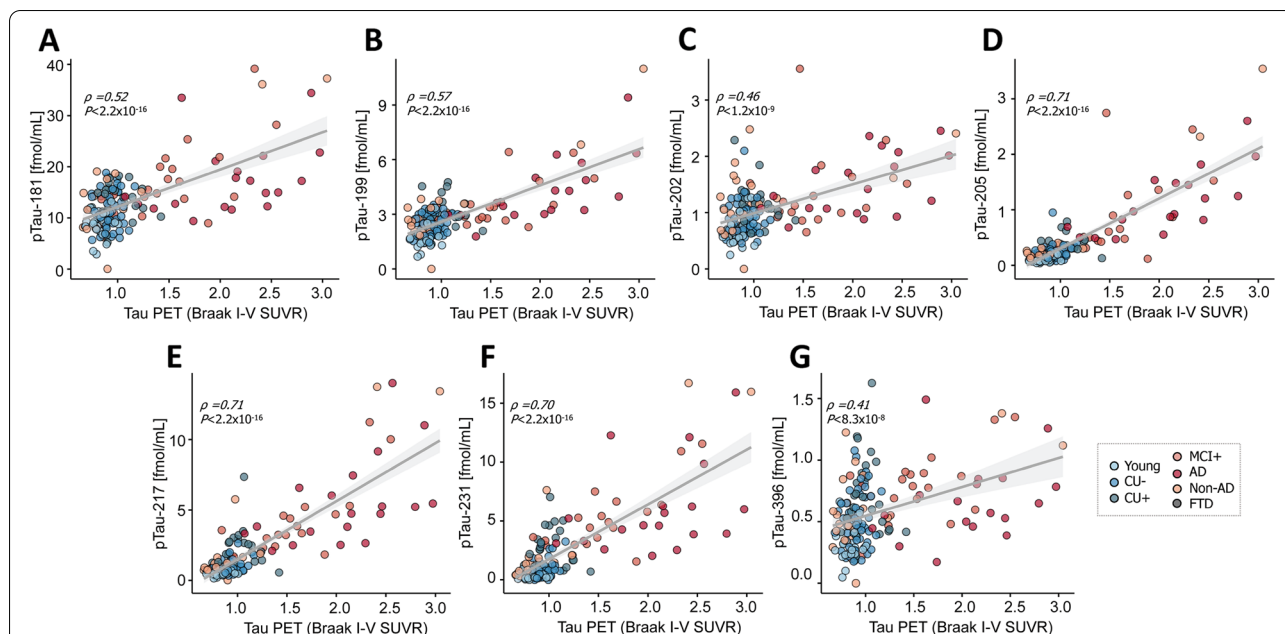


**Fig. 5** Correlation between the pTau biomarkers and tau PET (average SUVR of the regions corresponding to Braak stages I-IV) in the TRIAD cohort, for pTau-181 (A), pTau-199 (B), pTau-202 (C), pTau-205 (D), pTau-217 (E), pTau-231 (F) and pTau-396 (G) and tau pathology. Abbreviations: Aβ, amyloid-β; AD, Alzheimer’s disease; CU-, Aβ-negative cognitively unimpaired; CU+, Aβ-positive cognitively unimpaired; frontotemporal dementia; MCI+, Aβ-positive mild cognitive impairment; Non-AD, Aβ-negative “AD” dementia or mild cognitive impairment patients;  $\rho$ ,  $P$  value of the correlation test; PET, positron emission tomography;  $R$ , Spearman rank correlation coefficient; SUVR, standard uptake value ratio

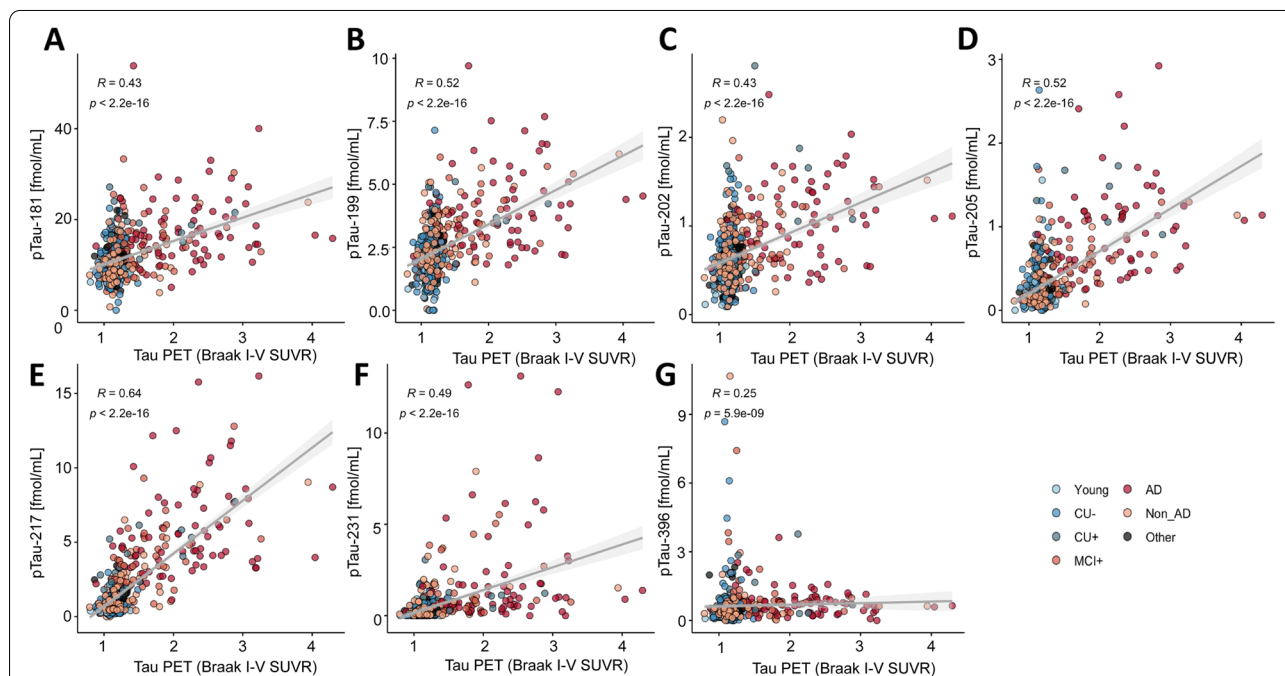


**Fig. 6** Correlation between the pTau biomarkers and tau PET (average SUVR of the regions corresponding to Braak stages I-IV) in the BioFINDER-2 cohort, for pTau-181 (A), pTau-199 (B), pTau-202 (C), pTau-205 (D), pTau-217 (E), pTau-231 (F) and pTau-396 (G) and tau pathology. Abbreviations: Aβ, amyloid-β; AD, Alzheimer’s disease; CU-, Aβ-negative cognitively unimpaired; CU+, Aβ-positive cognitively unimpaired; frontotemporal dementia; MCI+, Aβ-positive mild cognitive impairment; Non-AD, Aβ-negative “AD” dementia or mild cognitive impairment patients;  $R$ ,  $P$  value of the correlation test; PET, positron emission tomography;  $R$ , Spearman rank correlation coefficient; SUVR, standard uptake value ratio

## Discussion

Recent studies using ultrasensitive immunoassays indicate that different pTau species (pT181, pT217 and pT231) in plasma samples perform very well to identify AD, and correlate with both A $\beta$  and AD-type tau pathology as measured by PET [16, 20–22]. Studies showing very high (AUC 0.98) ability of plasma pT217 to discriminate Alzheimer's disease from other neurodegenerative disorders [43], stronger correlation of pT217 than pT181 with tau PET [14], CSF and IP-MS data showing a higher magnitude of increase of plasma pT217 and stronger association with A $\beta$  PET than pT181 [17], and CSF pT231 increasing at the early stage of the disease suggest that there may be disease associated differences across these pTau species and that measurement of specific phosphorylated species may be useful to track disease progression.

The PRM method described here is well suited to address this task as it enables multiple analytes to be measured in the same analytical run, thereby reducing analysis time, sample consumption, and importantly, also the effects of inter-run variation caused, e.g., by additional sample handling and freeze–thaw cycles. Furthermore, employing an antibody-independent sample preparation makes it possible to measure phosphorylation at potentially any site in tau.

The use of perchloric acid to purify tau by precipitating other sample proteins is well-established [44] and no studies have reported discrimination of specific processed or phosphorylated tau forms using this method. Absolute quantification of non-phosphorylated CSF tau using sample preparation based on perchloric acid precipitation has been previously reported [30, 45]. The high degree of correlation with Simoa data for pTau-181, pTau-217, and pTau-231 in our study is also an indication that there is no discrimination of any of the phospho-epitopes analyzed using the perchloric acid-based samples preparation. Perchloric acid-based sample preparation may thus be suitable to use in a reference method.

While IP-MS based methods can perform relative quantification, e.g., measuring the ratio of phosphorylated to non-phosphorylated peptide [28], absolute quantification presents a problem, as quantification is affected by the affinity of the used antibodies for the target protein. We found that the fold changes between Alzheimer's disease and CU- patients for the phosphorylation ratios, pS199/S199, pS202/S202, pT205/T205, and pT217/T217, were all smaller compared with the fold changes for the concentrations of the corresponding peptides themselves, quantified using the isotope-labelled internal standards (Supplementary Figure S6). This finding is logical when considering the large number of papers showing that levels pTau and total tau in CSF both are increased in Alzheimer's disease and correlate tightly.

We also found increased levels of tau phosphorylated at serine-396 in Alzheimer's disease compared with controls, in line with neuropathological evidence [46]. A major component of neurofibrillary tangles in Alzheimer's disease brains [47], Serine-396 is located at the extreme C-terminal part of the tau molecule. Previous studies have concluded that pTau-396 levels are not released into the CSF in quantities that are high enough to be reliably quantified, and so far only a single study published in 2002 reported increased levels of tau phosphorylated at 396 and/or 404 in CSF [9].

The PRM method also showed, in the discovery cohort, high diagnostic potential and differentiated between biomarker-positive Alzheimer's disease patients from biomarker-negative controls with up to 99% accuracy. We found marked increase of all phosphorylated tau species, with the highest increases observed for pT217, pT231 and pT205. Further, CSF levels of pT181, pT217 and pT231 correlated tightly ( $p < 0.001$ ) with Simoa measurements of the same pTau species using assays based on the N-terminal non-pTau antibody in the sandwich pair [16]. The correlations were also strong between the PRM measurements for the three peptides ( $\rho > 0.94$ ). Together, these findings support the LC–MS approach as a valid strategy to target multiple pTau biomarkers concurrently in the same sample.

The finding that both plasma and CSF pTau is truncated into N-terminal to mid-domain fragments [17], suggests that not only which pTau variant is captured, but also which pTau fragment is measured (as governed by the assay setup), may control the performance of pTau immunoassays as well as IP-MS methods. With our antibody-free PRM method, since short tryptic peptides encompassing each phosphorylated site are detected, all tau fragments that contain a given phosphopeptide are included in quantification, in effect, making quantification independent on proteolytic processing of tau. While this has the advantage of making the measured entity well defined, it may not be advantageous in terms of biomarker performance in all cases. For example, the reported presence in CSF of short endogenous tau peptides containing pT181 that are not increased in Alzheimer's disease [48], may decrease the performance of the PRM assay for this peptide, compared to pT181 immunoassays that require a longer tau fragment for detection.

## Conclusions

Our study confirms the tau phospho-epitopes pT231 and pT217 as markers of early Alzheimer's disease pathology, and identifies pT205 as a marker that increases in importance later in AD. The presented PRM method is the first antibody-independent method to measure pTau species in CSF, making it a potential candidate for future development of a reference method.

## Abbreviations

A $\beta$ : Amyloid beta; AUC: Area under the curve; CDR: Clinical Dementia Rating; CU: Cognitively unimpaired; FC: Fold change; GLM: Generalized linear model; HSD: Tukey honestly significant difference; IP: Immunoprecipitation; LC: Liquid chromatography; MCI: Mild cognitive impairment; MS: Mass spectrometry; PRM: Parallel reaction monitoring; pTau: Phospho-tau; ROC: Receiver operating curve; SUVR: Standardized uptake values ratio; tTau: Total tau.

## Supplementary Information

The online version contains supplementary material available at <https://doi.org/10.1186/s13024-022-00586-0>.

**Additional file 1: Supplementary Table S1.** Precursor and product ions used for quantification. **Supplementary Table S2.** Method reproducibility assessment. **Supplementary Table S3.** Performance of the pTau biomarkers in the biochemically characterized AD patients and controls. **Supplementary Table S4.** ROC curve analysis and fold-change to discriminate between amyloid positive and negative groups in TRIAD. **Supplementary Table S5.** ROC curve analysis and fold-change to discriminate between amyloid positive and negative groups in BioFINDER-2. **Supplementary Figure S1.** PRM chromatograms of the assayed tau phosphopeptides. **Supplementary Figure S2.** Scatter plots of phosphorylated peptide abundances in biochemically characterized AD patients and controls. **Supplementary Figure S3.** Correlations between the pTau PRM assay and Simoa immunoassay. **Supplementary Figure S4.** ROC curve analysis to discriminate between amyloid positive and negative groups in TRIAD. **Supplementary Figure S5.** ROC curve analysis to discriminate between amyloid positive and negative groups in BioFINDER-2. **Supplementary Figure S6.** Fold changes (AD versus CU-) for phospho-epitope concentrations compared with phosphorylation ratios.

## Acknowledgements

Not applicable.

## Authors' contributions

JG, HZ, KB conceived of the study; JG developed the LC-MS method; AB and NA analyzed data from the TRIAD cohort; NMC, NS and SJ analyzed data from the BioFINDER-2 cohort; LMG, MS, GB and JLR took part in method development and experimental work; SS, TP and PRN provided the TRIAD cohort; OH, NMC, NS and SJ provided the BioFINDER-2 cohort. All authors contributed to writing and proofreading the manuscript. The authors read and approved the final manuscript.

## Funding

Open access funding provided by University of Gothenburg. JG is supported by grants from Alzheimerfonden (#AF-930934) and Stiftelsen Gamla Tjänarinnor. HZ is a Wallenberg Scholar supported by grants from the Swedish Research Council (#2018-02532), the European Research Council (#681712), Swedish State Support for Clinical Research (#ALFGGB-720931), the Alzheimer Drug Discovery Foundation (ADDF), USA (#201809-2016862), the Alzheimer's disease Strategic Fund and the Alzheimer's Association (#ADSF-21-831376-C, #ADSF-21-831381-C and #ADSF-21-831377-C), the Olav Thon Foundation, the Erling-Persson Family Foundation, Stiftelsen för Gamla Tjänarinnor, Hjärtfonden, Sweden (#FO2019-0228), the European Union's Horizon 2020 research and innovation programme under the Marie Skłodowska-Curie grant agreement No 860197 (MIRIADE), and the UK Dementia Research Institute at UCL. KB is supported by the Swedish Research Council (#2017-00915), the Alzheimer Drug Discovery Foundation (ADDF), USA (#RDAPB-201809-2016615), the Swedish Alzheimer Foundation (#AF-742881), Hjärtfonden, Sweden (#FO2017-0243), the Swedish state under the agreement between the Swedish government and the County Councils, the ALF-agreement (#ALFGGB-715986), the European Union Joint Program for Neurodegenerative Disorders (JPND2019-466-236), and the National Institute of Health (NIH), USA, (grant #1R01AG068398-01). TTK is supported by the BrightFocus Foundation (#A2020812F), the Swedish Alzheimer Foundation (Alzheimerfonden; #AF-930627), the Swedish Brain Foundation (Hjärtfonden; #FO2020-0240), the Swedish Parkinson Foundation (Parkinsonfonden; #1252/20), the Swedish Dementia Foundation (Demensförbundet), Gamla Tjänarinnor Foundation,

the Aina (Ann) Wallströms and Mary-Ann Sjöbloms Foundation, the Agneta Prytz-Folkes & Gösta Folkes Foundation (#2020-00124), the Gun and Bertil Stohnes Foundation, and the Anna Lisa and Brother Björnsson's Foundation. The BioFINDER-2 study was supported by the Swedish Research Council (2016-00906), the Knut and Alice Wallenberg foundation (2017-0383), the Marianne and Marcus Wallenberg foundation (2015.0125), the Strategic Research Area MultiPark (Multidisciplinary Research in Parkinson's disease) at Lund University, the Swedish Alzheimer Foundation (AF-939932), the Swedish Brain Foundation (FO2021-0293), The Parkinson foundation of Sweden (1280/20), the Konung Gustaf V:s och Drottning Victorias Frimurarestiftelse, the Skåne University Hospital Foundation (2020-O000028), Regionalt Forskningsstöd (2020-0314) and the Swedish federal government under the ALF agreement (2018-Projekt0279).

## Availability of data and materials

Anonymized data will be shared by request from a qualified academic investigator for the sole purpose of replicating procedures and results presented in the article and as long as data transfer agrees with EU legislation on the general data protection regulation and decisions by the Ethical Review Board of the cohorts, which should be regulated in a material transfer agreement.

## Declarations

### Ethics approval and consent to participate

Permission to use CSF samples from the Clinical Routine Laboratory at the Sahlgrenska University Hospital, Mölndal, Sweden for method development was granted by the regional ethics committee in Gothenburg (August 11, 2014). The samples consisted of surplus CSF, which was left over from the routine clinical analysis, and were de-identified prior to use in this study to prevent the possibility to connect the samples to an individual. All participants of the TRIAD cohort included in this report provided written informed consent and the cohort studies were approved by REB from Douglas Hospital Research Centre—Montreal—Canada, no. IUSMD-16-60. Ethical permission to use CSF samples from the BioFINDER-2 cohort was given by the Regional Ethical Committee in Lund, Sweden.

### Consent for publication

Not applicable.

### Competing interests

HZ has served at scientific advisory boards and/or as a consultant for Alector, Eisai, Denali, Roche Diagnostics, Wave, Samumed, Siemens Healthineers, Pinteon Therapeutics, Nervgen, AZTherapies, CogRx and Red Abbey Labs, has given lectures in symposia sponsored by Cellectricon, Fujirebio, Alzecure and Biogen, and is a co-founder of Brain Biomarker Solutions in Gothenburg AB (BBS), which is a part of the GU Ventures Incubator Program. KB has served as a consultant, at advisory boards, or at data monitoring committees for Abcam, Axon, Biogen, JOMDD/Shimadzu, Julius Clinical, Lilly, MagQu, Novartis, Roche Diagnostics, and Siemens Healthineers, and is a co-founder of Brain Biomarker Solutions in Gothenburg AB (BBS), which is a part of the GU Ventures Incubator Program. OH has acquired research support (for the institution) from ADx, AVID Radiopharmaceuticals, Biogen, Eli Lilly, Eisai, Fujirebio, GE Healthcare, Pfizer, and Roche. In the past 2 years, he has received consultancy/speaker fees from AC Immune, Amylyx, Alzpath, BioArctic, Biogen, Cerveau, Fujirebio, Genentech, Novartis, Roche, and Siemens.

### Author details

<sup>1</sup>Department of Psychiatry and Neurochemistry, Institute of Neuroscience and Physiology, The Sahlgrenska Academy, University of Gothenburg, Gothenburg, Sweden. <sup>2</sup>Clinical Neurochemistry Laboratory, Sahlgrenska University Hospital, Mölndal, Sweden. <sup>3</sup>Translational Neuroimaging Laboratory, McGill Centre for Studies in Aging, McGill University, Montreal, QC, Canada. <sup>4</sup>Clinical Memory Research Unit, Faculty of Medicine, Lund University, Lund, Sweden. <sup>5</sup>Department of Neurology, Skåne University Hospital, Lund University, Lund, Sweden. <sup>6</sup>Wallenberg Centre for Molecular and Translational Medicine, University of Gothenburg, Gothenburg, Sweden. <sup>7</sup>King's College London, Institute of Psychiatry, Psychology & Neuroscience, Maurice Wohl Clinical Neuroscience Institute, London, UK. <sup>8</sup>NIHR Biomedical Research Centre for Mental Health & Biomedical Research Unit for Dementia at South London & Maudsley NHS Foundation, London, UK. <sup>9</sup>Department of Psychiatry, University of Pittsburgh,



Pittsburgh, PA, USA. <sup>10</sup>Department of Neurodegenerative Disease, UCL Institute of Neurology, Queen Square, London, UK. <sup>11</sup>UK Dementia Research Institute at UCL, London, UK. <sup>12</sup>Hong Kong Center for Neurodegenerative Diseases, Hong Kong, China. <sup>13</sup>Memory Clinic, Skåne University Hospital, Lund University, Lund, Sweden.

Received: 10 September 2022 Accepted: 25 November 2022

Published online: 12 December 2022

## References

- Grundke-Iqbal I, Iqbal K, Tung Y-C, Quinlan M, Wisniewski HM, Binder LI. Abnormal phosphorylation of the microtubule-associated protein tau (tau) in Alzheimer cytoskeletal pathology. *Proc Natl Acad Sci.* 1986;83(13):4913–7.
- DeTure MA, Dickson DW. The neuropathological diagnosis of Alzheimer's disease. *Mol Neurodegener.* 2019;14(1):32. <https://doi.org/10.1186/s13024-019-0333-5>.
- Iqbal K, Alonso Adel C, Chen S, et al. Tau pathology in Alzheimer disease and other tauopathies. *Biochim Biophys Acta.* 2005;1739(2–3):198–210.
- Blennow K, Hampel H, Weiner M, Zetterberg H. Cerebrospinal fluid and plasma biomarkers in Alzheimer disease. *Nat Rev Neurol.* 2010;6(3):131–44. <https://doi.org/10.1038/nrneurol.2010.4>.
- Skillback T, Rosen C, Asztely F, Mattsson N, Blennow K, Zetterberg H. Diagnostic performance of cerebrospinal fluid total tau and phosphorylated tau in Creutzfeldt-Jakob disease: results from the Swedish mortality registry. *JAMA Neurol.* 2014;71(4):476–83. <https://doi.org/10.1001/jamaneur.2013.6455>.
- Hesse C, Rosengren L, Andreassen N, et al. Transient increase in total tau but not phospho-tau in human cerebrospinal fluid after acute stroke. *Neurosci Lett.* 2001;297(3):187–90. [https://doi.org/10.1016/s0304-3940\(00\)01697-9](https://doi.org/10.1016/s0304-3940(00)01697-9).
- Buerger K, Zinkowski R, Teipel SJ, et al. Differential diagnosis of Alzheimer disease with cerebrospinal fluid levels of tau protein phosphorylated at threonine 231. *Arch Neurol.* 2002;59(8):1267–72. <https://doi.org/10.1001/archneur.59.8.1267>.
- Hampel H, Buerger K, Zinkowski R, et al. Measurement of phosphorylated tau epitopes in the differential diagnosis of Alzheimer disease: a comparative cerebrospinal fluid study. *Arch Gen Psychiatry.* 2004;61(1):95–102. <https://doi.org/10.1001/archpsyc.61.1.95>.
- Hu YY, He SS, Wang X, et al. Levels of nonphosphorylated and phosphorylated tau in cerebrospinal fluid of Alzheimer's disease patients: an ultrasensitive bienzyme-substrate-recycle enzyme-linked immunosorbent assay. *Am J Pathol.* 2002;160(4):1269–78. [https://doi.org/10.1016/S0002-9440\(10\)62554-0](https://doi.org/10.1016/S0002-9440(10)62554-0).
- Ishiguro K, Ohno H, Arai H, et al. Phosphorylated tau in human cerebrospinal fluid is a diagnostic marker for Alzheimer's disease. *Neurosci Lett.* 1999;270(2):91–4. [https://doi.org/10.1016/s0304-3940\(99\)00476-0](https://doi.org/10.1016/s0304-3940(99)00476-0).
- Kohnken R, Buerger K, Zinkowski R, et al. Detection of tau phosphorylated at threonine 231 in cerebrospinal fluid of Alzheimer's disease patients. *Neurosci Lett.* 2000;287(3):187–90. [https://doi.org/10.1016/s0304-3940\(00\)01178-2](https://doi.org/10.1016/s0304-3940(00)01178-2).
- Meredith JE Jr, Sankaranarayanan S, Guss V, et al. Characterization of novel CSF Tau and ptau biomarkers for Alzheimer's disease. *PLoS ONE.* 2013;8(10):e76523. <https://doi.org/10.1371/journal.pone.0076523>.
- Singer D, Soininen H, Alafuzoff I, Hoffmann R. Immuno-PCR-based quantification of multiple phosphorylated tau-epitopes linked to Alzheimer's disease. *Anal Bioanal Chem.* 2009;395(7):2263–7. <https://doi.org/10.1007/s00216-009-3208-8>.
- Janelidze S, Stomrud E, Smith R, et al. Cerebrospinal fluid p-tau217 performs better than p-tau181 as a biomarker of Alzheimer's disease. *Nat Commun.* 2020;11(1):1683. <https://doi.org/10.1038/s41467-020-15436-0>.
- Karikari TK, Emersic A, Vrillon A, et al. Head-to-head comparison of clinical performance of CSF phospho-tau T181 and T217 biomarkers for Alzheimer's disease diagnosis. *Alzheimers Dement.* 2021;17(5):755–67. <https://doi.org/10.1002/alz.12236>.
- Suarez-Calvet M, Karikari TK, Ashton NJ, et al. Novel tau biomarkers phosphorylated at T181, T217 or T231 rise in the initial stages of the preclinical Alzheimer's continuum when only subtle changes in Aβ pathology are detected. *EMBO Mol Med.* 2020;12(12):e12921. <https://doi.org/10.15252/emmm.202012921>.
- Barthelemy NR, Li Y, Joseph-Mathurin N, et al. A soluble phosphorylated tau signature links tau, amyloid and the evolution of stages of dominantly inherited Alzheimer's disease. *Nat Med.* 2020;26(3):398–407. <https://doi.org/10.1038/s41591-020-0781-z>.
- Augustinack JC, Schneider A, Mandelkow EM, Hyman BT. Specific tau phosphorylation sites correlate with severity of neuronal cytopathology in Alzheimer's disease. *Acta Neuropathol.* 2002;103(1):26–35. <https://doi.org/10.1007/s004010100423>.
- Benussi A, Karikari TK, Ashton NJ, et al. Diagnostic and prognostic value of serum NfL and p-Tau181 in frontotemporal lobar degeneration. *J Neurol Neurosurg Psychiatry.* 2020;91(9):960–7. <https://doi.org/10.1136/jnnp-2020-323487>.
- Karikari TK, Benedet AL, Ashton NJ, et al. Diagnostic performance and prediction of clinical progression of plasma phospho-tau181 in the Alzheimer's Disease Neuroimaging Initiative. *Mol Psychiatry.* 2021;26(2):429–42. <https://doi.org/10.1038/s41380-020-00923-z>.
- O'Connor A, Karikari TK, Poole T, et al. Plasma phospho-tau181 in presymptomatic and symptomatic familial Alzheimer's disease: a longitudinal cohort study. *Mol Psychiatry.* 2020. <https://doi.org/10.1038/s41380-020-0838-x>.
- Rodriguez JL, Karikari TK, Suarez-Calvet M, et al. Plasma p-tau181 accurately predicts Alzheimer's disease pathology at least 8 years prior to post-mortem and improves the clinical characterisation of cognitive decline. *Acta Neuropathol.* 2020;140(3):267–78. <https://doi.org/10.1007/s00401-020-02195-x>.
- Hanger DP, Betts JC, Loviny TL, Blackstock WP, Anderton BH. New phosphorylation sites identified in hyperphosphorylated tau (paired helical filament-tau) from Alzheimer's disease brain using nanoelectrospray mass spectrometry. *J Neurochem.* 1998;71(6):2465–76. <https://doi.org/10.1046/j.1471-4159.1998.71062465.x>.
- Hanger DP, Byers HL, Wray S, et al. Novel phosphorylation sites in tau from Alzheimer brain support a role for casein kinase 1 in disease pathogenesis. *J Biol Chem.* 2007;282(32):23645–54. <https://doi.org/10.1074/jbc.M703269200>.
- Hasegawa M, Morishima-Kawashima M, Takio K, Suzuki M, Titani K, Ihara Y. Protein sequence and mass spectrometric analyses of tau in the Alzheimer's disease brain. *J Biol Chem.* 1992;267(24):17047–54.
- Sjogren M, Vanderstichele H, Agren H, et al. Tau and Aβ42 in cerebrospinal fluid from healthy adults 21–93 years of age: establishment of reference values. *Clin Chem.* 2001;47(10):1776–81.
- Portelius E, Hansson SF, Tran AJ, et al. Characterization of tau in cerebrospinal fluid using mass spectrometry. *J Proteome Res.* 2008;7(5):2114–20. <https://doi.org/10.1021/pr7008669>.
- Barthelemy NR, Mallipeddi N, Moiseyev P, Sato C, Bateman RJ. Tau phosphorylation rates measured by mass spectrometry differ in the intracellular brain vs. extracellular cerebrospinal fluid compartments and are differentially affected by Alzheimer's disease. *Front Aging Neurosci.* 2019;11:121. <https://doi.org/10.3389/fnagi.2019.00121>.
- Barthelemy NR, Gabelle A, Hirtz C, et al. Differential mass spectrometry profiles of tau protein in the cerebrospinal fluid of patients with Alzheimer's disease, progressive supranuclear palsy, and dementia with Lewy bodies. *J Alzheimers Dis.* 2016;51(4):1033–43. <https://doi.org/10.3233/JAD-150962>.
- Bros P, Vialaret J, Barthelemy N, et al. Antibody-free quantification of seven tau peptides in human CSF using targeted mass spectrometry. *Front Neurosci.* 2015;9:302. <https://doi.org/10.3389/fnins.2015.00302>.
- McKhann GM, Knopman DS, Chertkow H, et al. The diagnosis of dementia due to Alzheimer's disease: recommendations from the national institute on aging-Alzheimer's association workgroups on diagnostic guidelines for Alzheimer's disease. *Alzheimers Dement.* 2011;7(3):263–9. <https://doi.org/10.1016/j.jalz.2011.03.005>.
- Hansson O, Palmqvist S. The Swedish BIOFINDER Study. <https://biofinder.se/>.
- Edition F. Diagnostic and statistical manual of mental disorders. *Am Psychiatric Assoc.* 2013;21:591–643.
- Jack CR Jr, Bennett DA, Blennow K, et al. NIA-AA research framework: toward a biological definition of Alzheimer's disease. *Alzheimers Dement.* 2018;14(4):535–62.
- Gelb DJ, Oliver E, Gilman S. Diagnostic criteria for Parkinson disease. *Arch Neurol.* 1999;56(1):33–9.

36. Höglinger GU, Respondek G, Stamelou M, et al. Clinical diagnosis of progressive supranuclear palsy: the movement disorder society criteria. *Mov Disord*. 2017;32(6):853–64.
37. Gilman S, Wenning G, Low PA, et al. Second consensus statement on the diagnosis of multiple system atrophy. *Neurology*. 2008;71(9):670–6.
38. Gorno-Tempini ML, Hillis AE, Weintraub S, et al. Classification of primary progressive aphasia and its variants. *Neurology*. 2011;76(11):1006–14.
39. Folstein MF, Folstein SE, McHugh PR. "Mini-mental state": a practical method for grading the cognitive state of patients for the clinician. *J Psychiatr Res*. 1975;12(3):189–98.
40. Palmqvist S, Janelidze S, Quiroz YT, et al. Discriminative accuracy of plasma phospho-tau217 for Alzheimer disease vs other neurodegenerative disorders. *JAMA*. 2020;324(8):772–81.
41. Ashton NJ, Pascoal TA, Karikari TK, et al. Plasma p-tau231: a new biomarker for incipient Alzheimer's disease pathology. *Acta Neuropathol*. 2021;141(5):709–24. <https://doi.org/10.1007/s00401-021-02275-6>.
42. Pascoal TA, Theriault J, Benedet AL, et al. 18F-MK-6240 PET for early and late detection of neurofibrillary tangles. *Brain*. 2020;143(9):2818–30. <https://doi.org/10.1093/brain/awaa180>.
43. Palmqvist S, Janelidze S, Quiroz YT, et al. Discriminative Accuracy of Plasma Phospho-tau217 for Alzheimer Disease vs Other Neurodegenerative Disorders. *Jama-J Am Med Assoc*. 2020;324(8):772–81. <https://doi.org/10.1001/jama.2020.12134>.
44. Lindwall G, Cole RD. The purification of tau protein and the occurrence of two phosphorylation states of tau in brain. *J Biol Chem*. 1984;259(19):12241–5.
45. Barthelemy NR, Fenaille F, Hirtz C, et al. Tau protein quantification in human cerebrospinal fluid by targeted mass spectrometry at high sequence coverage provides insights into its primary structure heterogeneity. *J Proteome Res*. 2016;15(2):667–76. <https://doi.org/10.1021/acs.jproteome.5b01001>.
46. Mondragon-Rodriguez S, Perry G, Luna-Munoz J, Acevedo-Aquino MC, Williams S. Phosphorylation of tau protein at sites Ser(396–404) is one of the earliest events in Alzheimer's disease and Down syndrome. *NeuroPath Appl Neuro*. 2014;40(2):121–35. <https://doi.org/10.1111/nan.12084>.
47. Hanger DP, Anderton BH, Noble W. Tau phosphorylation: the therapeutic challenge for neurodegenerative disease. *Trends Mol Med*. 2009;15(3):112–9. <https://doi.org/10.1016/j.molmed.2009.01.003>.
48. Hansson K, Dahlen R, Hansson O, et al. Use of the tau protein-to-peptide ratio in CSF to improve diagnostic classification of Alzheimer's disease. *Clin Mass Spectrom*. 2019;14:74–82. <https://doi.org/10.1016/j.clinms.2019.07.002>.

## Publisher's Note

Springer Nature remains neutral with regard to jurisdictional claims in published maps and institutional affiliations.

Ready to submit your research? Choose BMC and benefit from:

- fast, convenient online submission
- thorough peer review by experienced researchers in your field
- rapid publication on acceptance
- support for research data, including large and complex data types
- gold Open Access which fosters wider collaboration and increased citations
- maximum visibility for your research: over 100M website views per year

At BMC, research is always in progress.

Learn more [biomedcentral.com/submissions](https://biomedcentral.com/submissions)

